www.sciencemag.org/cgi/content/full/science.aar6245/DC1

# Supplementary Materials for

## CRISPR-Cas12a target binding unleashes indiscriminate single-stranded DNase activity

Janice S. Chen,* Enbo Ma,* Lucas B. Harrington,* Maria Da Costa, Xinran Tian, Joel M. Palefsky, Jennifer A. Doudna†

*These authors contributed equally to this work.
†Corresponding author. Email: doudna@berkeley.edu

Published 15 February 2018 on *Science* First Release
DOI: 10.1126/science.aar6245

**This PDF file includes:**

Materials and Methods
Figs. S1 to S15
Table S1
References

## Materials and Methods

**Protein expression and purification.** DNA sequences encoding SpCas9 and Cas12 proteins and mutants were cloned into a custom pET-based expression vector containing an N-terminal 10×His-tag, maltose-binding protein (MBP) and TEV protease cleavage site. Point mutations were introduced by around-the-horn PCR and verified by DNA sequencing. Proteins were purified as described (*35*), with the following modifications: *E. coli* BL21(DE3) containing SpCas9 or Cas12 expression plasmids were grown in Terrific Broth at 16°C for 14 hr. Cells were harvested and resuspended in Lysis Buffer (50 mM Tris-HCl, pH 7.5, 500 mM NaCl, 5% (v/v) glycerol, 1 mM TCEP, 0.5 mM PMSF and 0.25 mg/ml lysozyme), disrupted by sonication, and purified using Ni-NTA resin. After overnight TEV cleavage at 4°C, proteins were purified over an MBPTrap HP column connected to a HiTrap Heparin HP column for cation exchange chromatography. The final gel filtration step (Superdex 200) was carried out in elution buffer containing 20 mM Tris-HCl, pH 7.5, 200 mM NaCl (or 250 mM NaCl for AaCas12b), 5% (v/v) glycerol and 1 mM TCEP. All proteins tested in this study are shown in **fig. S1**.

**Nucleic acid preparation.** DNA substrates were synthesized commercially (IDT). For FQ-reporter assays, activator DNA duplexes were prepared by annealing 5-fold molar excess of the NTS to TS in 1× hybridization buffer (20 nM Tris-Cl, pH 7.5, 100 mM KCl, 5 mM $MgCl_2$), heating at 95°C and slow-cooling on the benchtop. HPV16 and HPV18 fragments were synthesized as gBlocks (IDT) and cloned into a custom pET-based vector via Gibson assembly. Plasmid DNA for titration experiments was quantified using a Qubit fluorometer (Invitrogen). For radiolabeled cleavage assays, PAGE-purified DNA oligos were prepared as described.

sgRNA templates were PCR amplified from a pUC19 vector or overlapping primers containing a T7 promoter, 20 nucleotide target sequence and an sgRNA scaffold. The amplified

PCR product served as the DNA template for *in vitro* transcription reactions, which were performed as described (*35*). crRNAs were transcribed *in vitro* using a single-stranded DNA template containing a T7 promoter, repeat and spacer in the reverse complement orientation, which was annealed to T7 forward primer in 1× hybridization buffer. All DNA and RNA substrates are listed in **Table S1**.

**DNA cleavage assays.** Generally, Cas12a-mediated cleavage assays were carried out in cleavage buffer consisting of 20 mM HEPES (pH 7.5), 150 mM KCl, 10 mM $MgCl_2$, 1% glycerol and 0.5 mM DTT. For M13-targeting assays, 30 nM Cas12a was pre-assembled with either 36 nM of M13-targeting crRNA (*cis*) or with 36 nM of crRNA and 40 nM complementary ssDNA (activator) with no sequence homology to M13 (*trans*) at 37°C for 10 min. The reaction was initiated by adding 10 nM M13mp18 ssDNA (New England Biolabs) and incubated at 37°C for indicated timepoints. Reactions were quenched with DNA loading buffer (30% (v/v) glycerol, 0.25% (w/v) bromophenol blue, 0.25% (w/v) xylene cyanol) containing 15 mM EDTA and separated by 1.5% agarose gel pre-stained with SYBER Gold (Invitrogen).

For radiolabeled cleavage assays, the substrates used were 5′-end-labeled with T4 PNK (NEB) in the presence of gamma $^{32}$P-ATP. For dsDNA substrates, the non-target strand was first 5′-end-labeled and then annealed with excess corresponding target strand. The concentrations of Cas12a (or SpCas9), guide RNA and $^{32}$P-labeled substrates used in the reaction were 30 nM, 36 nM and 1–3 nM (unless otherwise stated), respectively. Reactions were incubated for 30 min (unless otherwise stated) at 37°C (or 47.5°C for the thermophilic AacCas12b) and quenched with formamide loading buffer (final concentration 45% formamide and 15 mM EDTA, with trace amount of xylene cyanol and bromophenol blue) for 2-3 min at 90°C. The substrates and

products were resolved by 12% urea-denaturing PAGE gel and quantified with Amersham Typhoon (GE Healthcare).

For substrate turnover studies, the pre-assembled Cas12a-crRNA or Cas12a-crRNA-activator (target ssDNA or dsDNA) were incubated at 37°C for 10 min, and 30 nM of the pre-assembled RNP were used for each reaction with various substrate concentrations at 15, 30, 45, and 60 nM, respectively.

**Fluorophore quencher (FQ)-labeled reporter assays.** LbCas12a-crRNA complexes were pre-assembled by incubating 200 nM LbCpf1 with 250 nM crRNA and 4 nM activator (ssDNA, dsDNA or ssRNA) at 37°C for 30 min. The reaction was initiated by diluting LbCas12a complexes to a final concentration of 50 nM LbCas12a : 62.5 nM crRNA : 1 nM activator in a solution containing 1× Binding Buffer (20 mM Tris-HCl, pH 7.5, 100 mM KCl, 5 mM $MgCl_2$, 1 mM DTT, 5% glycerol, 50 μg $ml^{-1}$ heparin) and 50 nM DNaseAlert substrate™ (IDT) or custom ssDNA/ssRNA FQ reporter substrates in a 20 μl reaction **(Table S1)**. HPV detection assays were performed as above, with the following modifications: LbCas12a was pre-assembled with an HPV16 or HPV18-targeting crRNA and diluted in a solution containing 1× Binding Buffer, custom ssDNA-FQ reporter and 1, 10, 100, or 1000 nM of HPV16- or HPV18-containing plasmids. Reactions (20 μl, 384-well microplate format) were incubated in a fluorescence plate reader (Tecan Infinite Pro F200) for up to 120 minutes at 37°C with fluorescence measurements taken every 30 seconds (DNaseAlert substrate = $\lambda_{ex}$: 535 nm; $\lambda_{em}$: 595 nm, custom ssDNA/ssRNA FQ substrates = $\lambda_{ex}$: 485 nm; $\lambda_{em}$: 535 nm).

For *trans*-cleavage rate determination, background-corrected fluorescence values were calculated by subtracting fluorescence values obtained from reactions carried out in the absence of target plasmid. The resulting data were fit to a single exponential decay curve (GraphPad

Software), according to the following equation: Fraction cleaved = $A \times (1 - \exp(-k \times t))$, where A is the amplitude of the curve, k is the first-order rate constant, and t is time.

For Michaelis-Menten analysis, LbCas12a-crRNA-activator (target ssDNA or dsDNA) complexes were prepared as described above, and reaction was initiated by diluting LbCas12a complexes to a final concentration of 5 nM LbCas12a : 6.25 nM crRNA : 0.1 nM activator (effective complex = 0.1 nM) in a solution containing 1× Binding Buffer and 0.001, 0.01, 0.1, 0.2, 0.5, 1 or 2 uM of DNaseAlert™ substrate (IDT). Reactions were incubated in a fluorescence plate reader for up to 30 minutes at 37°C with fluorescence measurements taken every 30 seconds ($\lambda_{ex}$: 535 nm; $\lambda_{em}$: 595 nm). The initial velocity ($V_0$) was calculated by fitting to a linear regression and plotted against the substrate concentration to determine the Michaelis-Menten constants (GraphPad Software), according to the following equation: $Y = (V_{max} \times X)/(K_m + X)$, where X is the substrate concentration and Y is the enzyme velocity. The turnover number ($k_{cat}$) was determined by the following equation: $k_{cat} = V_{max}/E_t$, where $E_t = 0.1$ nM.

**Human clinical sample collection and DNA preparation.** Anal sample donors were recruited from the UCSF Anal Neoplasia Clinic, Research and Education Center (ANCRE). The study was approved by the UCSF Committee on Human Research. After informed consent was obtained, participants had an anal swab inserted into a Thinprep™ vial for anal cytology and HPV testing. Cell suspension left over from the first swab after monolayer cytology slides were made was used for HPV DNA PCR.

A crude DNA preparation was made by pelleting 1.5 ml of the cell suspension. After the pellet was allowed to dry, it was suspended in 100 µl Tris-EDTA with proteinase K (Life Technologies) at a concentration of 200 µg/ml and incubated at 56°C for 1 hour, then the proteinase K was heat inactivated. Five µl of this was used in the HPV consensus PCR. DNA

preparation from human cell lines (SiHa, HeLa, BJAB) was performed as above, with the following modifications: $10^6$–$10^7$ cells were harvested, resuspended in 100 µl Tris-EDTA with proteinase K, incubated at 56°C for 1 hour, then the proteinase K was heat inactivated. One µl of this sample was used for DETECTR experiments.

**DETECTR assays.** DETECTR combines Recombinase Polymerase Amplification (RPA) using TwistAmp Basic (Twist Biosciences) followed by Cas12a detection in the same reaction. Briefly, 50 µl reactions containing 1 µl sample, 0.48 µM forward and reverse primer, 1× rehydration buffer, 14 mM magnesium acetate and RPA mix were incubated at 37°C for 10 minutes. The RPA reaction (18 µl) was transferred to a 384-well microplate and 50 nM LbCas12a : 62.5 nM crRNA : 50 nM custom ssDNA-FQ reporter was added directly to the reaction (20 µl final volume). Reactions were incubated in a fluorescence plate reader (Tecan Infinite Pro F200) for 1–2h at 37°C with fluorescence measurements taken every minute ($\lambda_{ex}$: 485 nm; $\lambda_{em}$: 535 nm).

For HPV identification by DETECTR, detection values of HPV types 16 or 18 in human samples were normalized to the maximum mean fluorescence signal obtained using LbCas12a-crRNA targeting the hypervariable loop V of the L1 gene within HPV16 or HPV18 (*36*). A one-way ANOVA with Dunnett's post test was used to determine the positive cutoff (set at $p \leq 0.05$) for identification of HPV16 or HPV18 in patient samples. Based on this cutoff, 100% of samples were accurately identified for HPV16 infection (25/25 agreement with PCR-based results), while 92% of samples were accurately identified for HPV18 infection (23/25 agreement with PCR-based results).

**HPV genotyping and validation.**

PCR was performed as described previously (*28, 37*) using a modified pool of MY09/MY11 consensus HPV L1 primers as well as primers for amplification of the human beta-

globin as an indicator of specimen adequacy as described previously (*28*). After 40 amplification cycles, specimens were probed with a biotin-labeled HPV L1 consensus probe mixture. A separate membrane was probed with a biotin-labeled probe to the human beta-globin gene. Specimens were typed by hybridizing to 38 different HPV types, 6/11, 16, 18, 26/69, 30, 31, 32/42, 33, 34, 35, 39, 45, 51, 52, 53, 54, 56, 57/2/27, 58, 59, 61, 62, 66, 67, 68, 70, 71, 72, 73, 81, 82, 83, 84, 85, 86/87, 90/106, 97, 102/89, as well as two separate mixtures. Mix1 contains 7, 13, 40, 43, 44, 55, 74, and 91, and Mix 2 contains 3, 10, 28, 29, 77, 78, and 94. Specimens negative for beta-globin gene amplification were excluded from analysis. The results of PCR were recorded on a scale from 0 to 5 based on the intensity of the signal on the dot-blots, as described previously (*37*). Samples with results recorded as 1 or more were considered to be positive.

**Supplementary Figures S1-S15**

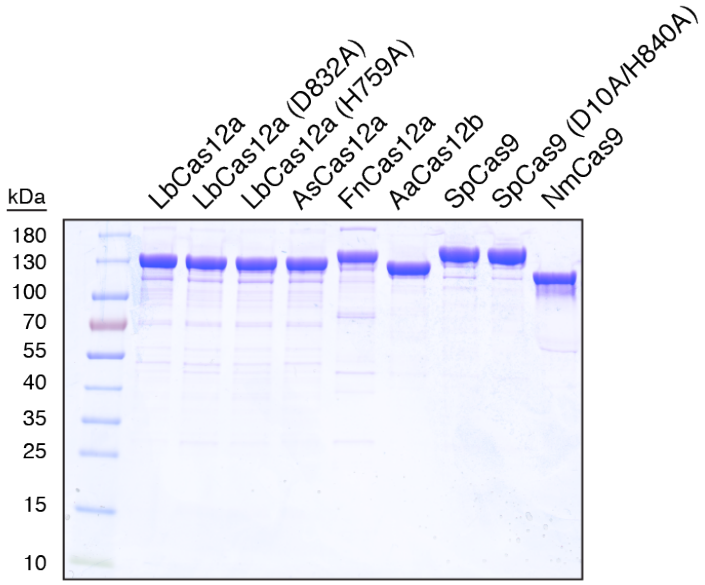



**Fig. S1**

**Purification of Cas12 and Cas9 proteins.** SDS-PAGE gel of all purified Cas12 and Cas9 proteins used in this study.

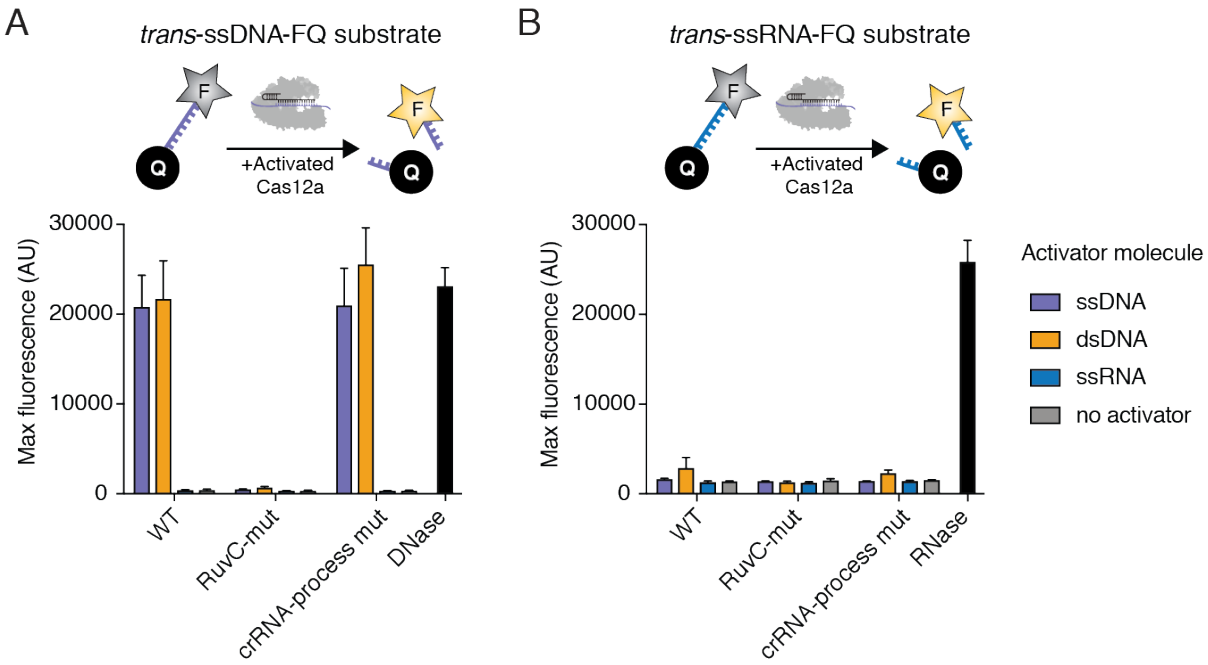



**Fig. S2**

**LbCas12a is a DNA-activated general DNase.** Quantification of maximum fluorescence signal generated after incubating LbCas12a-crRNA-activator with a custom (**A**) *trans*-ssDNA-FQ or (**B**) *trans*-ssRNA-FQ reporter for 1h at 37°C, with DNase I or RNase A controls where indicated. Error bars represent the mean ± s.d., where $n = 3$ replicates.

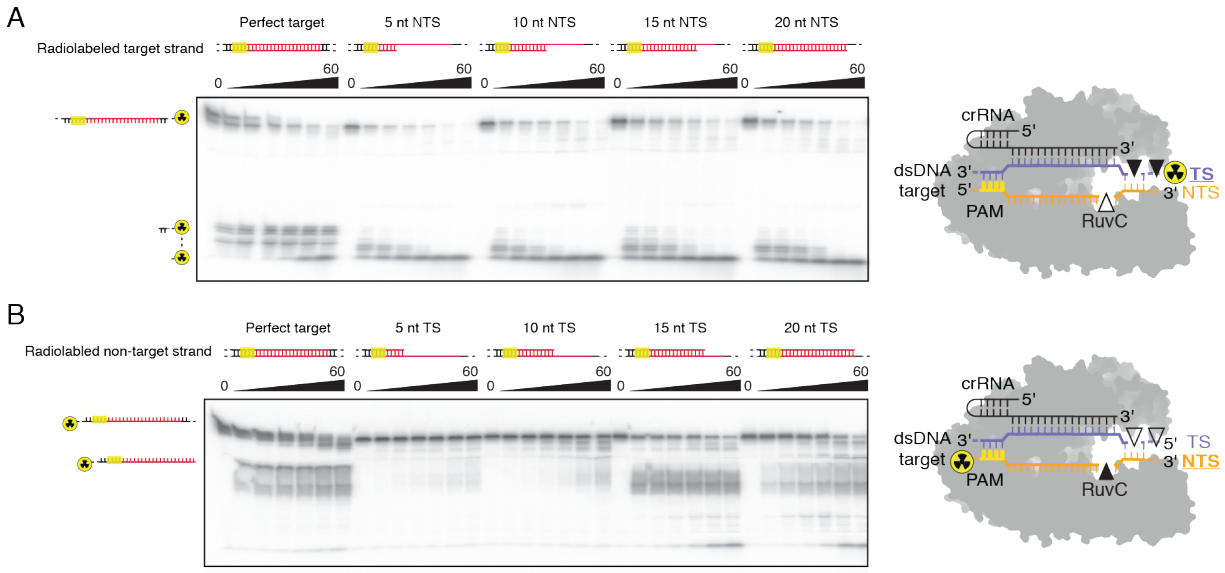



**Fig. S3**

**Target strand recognition is a pre-requisite for single-stranded DNA cleavage.** Cleavage timecourse assays using LbCas12a with (**A**) truncated non-target strand (NTS) annealed to a radiolabeled target strand (TS), (**B**) truncated TS annealed to a radiolabeled NTS. Timecourses represent minutes and cleavage products are resolved by denaturing PAGE. Schematic on right depicts cleavage of the radiolabeled TS (**A**) or NTS (**B**), which generates a Cas12a-mediated staggered cut.

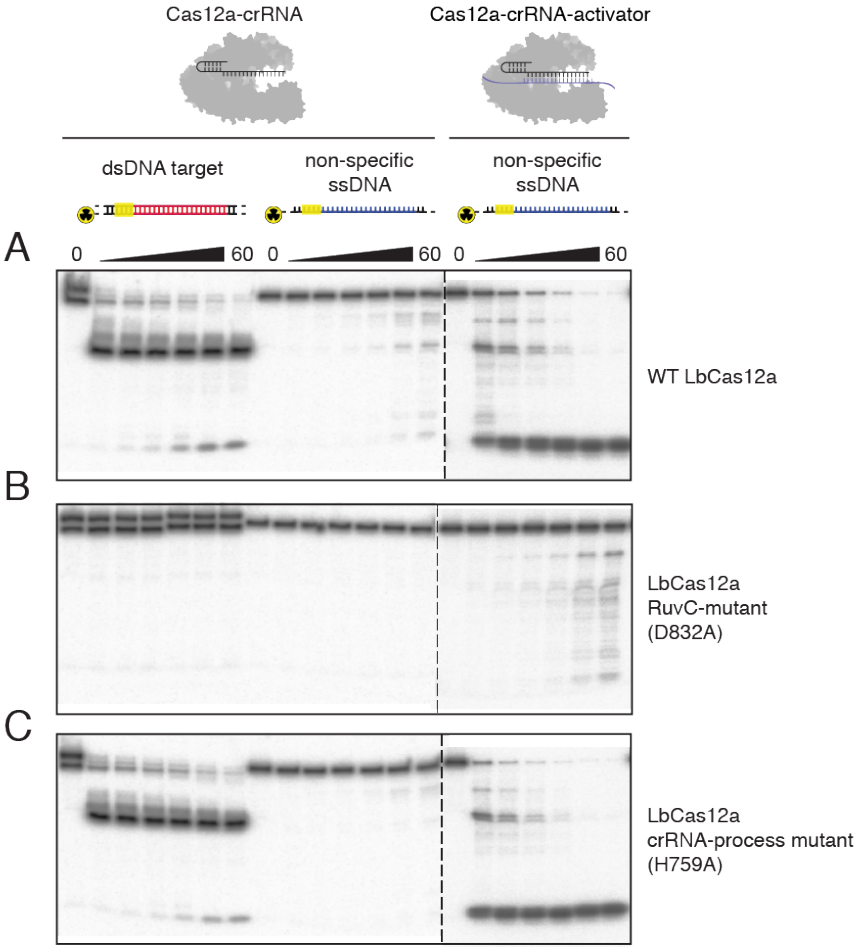



**Fig. S4**

**The RuvC nuclease domain is responsible for activator-dependent, non-specific DNase activity.** Cleavage timecourse gel with radiolabeled non-target strand of a complementary dsDNA and non-specific ssDNA substrate using (**A**) WT LbCas12a, (**B**) RuvC catalytic mutant (D832A) and (**C**) crRNA-processing mutant (H759A), with or without a ssDNA activator. Timecourses represent minutes and cleavage products are resolved by denaturing PAGE.

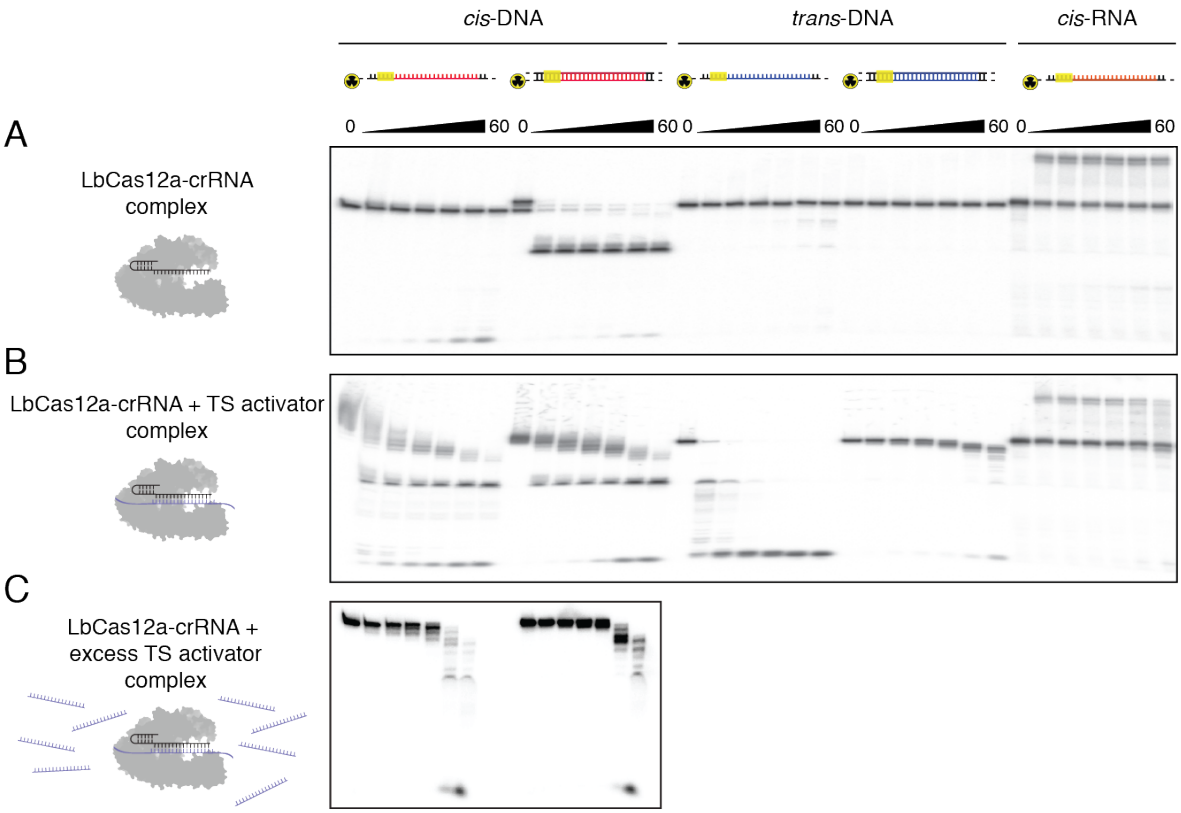



**Fig. S5**

**LbCas12a *trans*-cleavage degrades complementary and non-specific ssDNA, but not ssRNA.** Cleavage timecourse gels of LbCas12a-crRNA complexes using (**A**) no activator, (**B**) ssDNA activator in 1.2-fold molar excess, or (**C**) ssDNA activator in 100-fold molar excess. The observed cleavage of the *cis*-dsDNA in (**B**) and (**C**) may result from the short 55 bp duplexed substrates undergoing local DNA melting that subsequently exposes free ssDNA ends, consistent with the cleavage pattern. In a genomic context, we speculate that cis-dsDNA cleavage is not relevant given that the target sequence is embedded within long stretches of dsDNA, but this *in vitro* observation warrants further investigation. Radiolabeled substrates are indicated, where *cis* indicates a complementary target and *trans* indicates a non-complementary sequence. For *cis*

substrates, the non-target strand is radiolabeled. Timecourses represent minutes and cleavage products are resolved by denaturing PAGE.

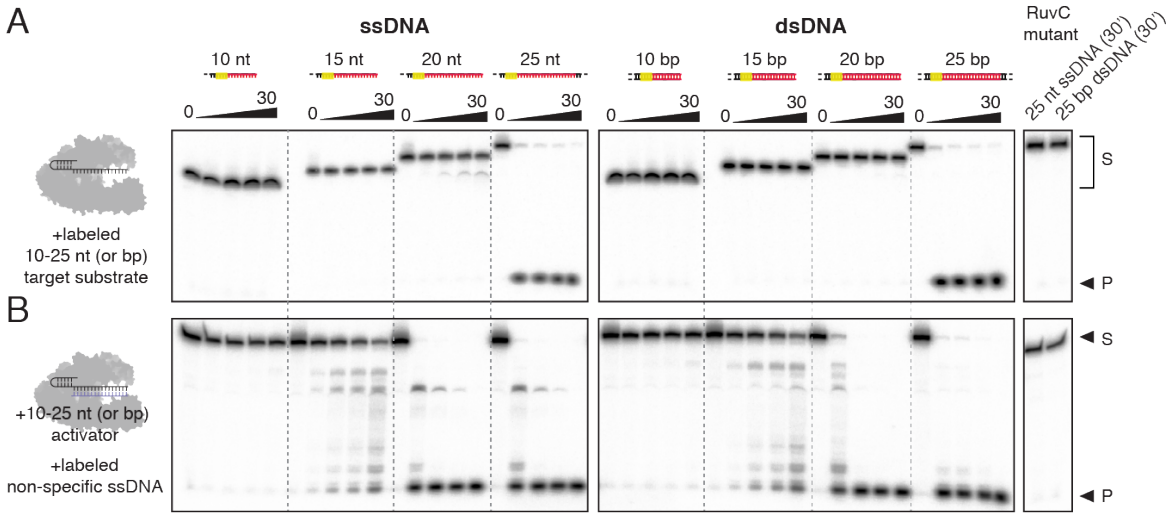
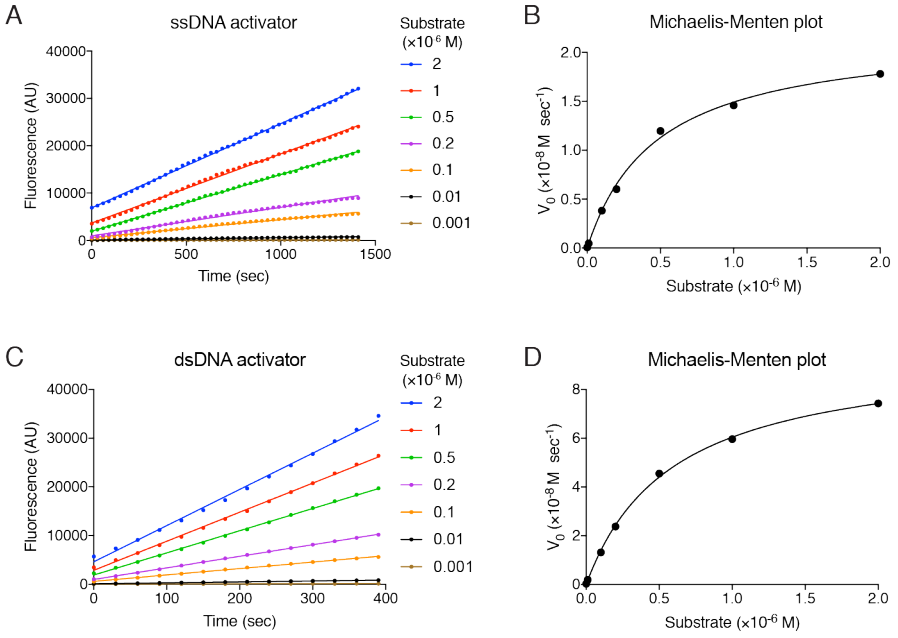



**Fig. S6**

**Target strand cleavage by Cas12a is not required for triggering non-specific ssDNase activity.** Cleavage timecourse assays using LbCas12a with (**A**) radiolabeled target strand with either a ssDNA (10-25 nt) or dsDNA (10-25 bp) substrate, or (**B**) radiolabeled non-specific ssDNA substrate in the presence of either a ssDNA (10-25 nt) or dsDNA (10-25 bp) activator. Timecourses represent minutes and cleavage products are resolved by denaturing PAGE.




E

| Activator | $k_{cat}$ ($sec^{-1}$) | $K_m$ ($M^{-1}$) | $k_{cat}/K_m$ ($sec^{-1}\ M^{-1}$) |
|---|---|---|---|
| ssDNA | $2.50 \pm 0.30 \times 10^{2}$ | $4.94 \pm 0.16 \times 10^{-7}$ | $5.10 \pm 0.47 \times 10^{8}$ |
| dsDNA | $1.25 \pm 0.27 \times 10^{3}$ | $7.25 \pm 1.74 \times 10^{-7}$ | $1.73 \pm 0.18 \times 10^{9}$ |

**Fig. S7**

**Michaelis-Menten analysis reveals robust *trans*-cleavage activity with a ssDNA and dsDNA activator.** Representative plots of initial velocity versus time for a (**A**) ssDNA or (**C**) dsDNA activator, using 0.1 nM effective LbCas12a-crRNA-activator complex and increasing DNaseAlert substrate concentrations at 37°C. Michaelis-Menten fits for the corresponding (**B**) ssDNA or (**D**) dsDNA activator. (**E**) Calculated $k_{cat}$, $K_m$ and $k_{cat}/K_m$ values report the mean ± s.d., where $n = 3$ replicates.

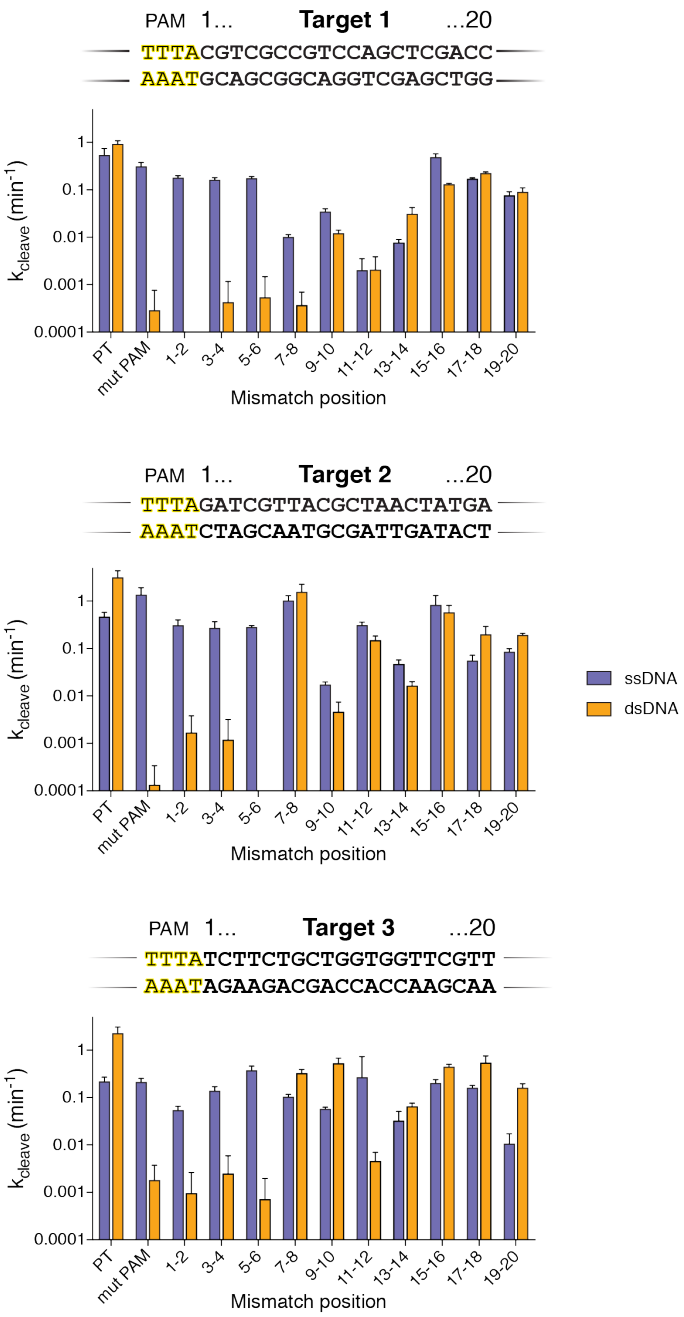



**Fig. S8**

**The PAM sequence and PAM-proximal mismatches in a dsDNA activator provide specificity for *trans*-activation.** Quantification of *trans*-cleavage kinetics using mismatched substrates for three distinct target sequences; error bars represent the mean ± s.d., where $n = 3$ replicates.

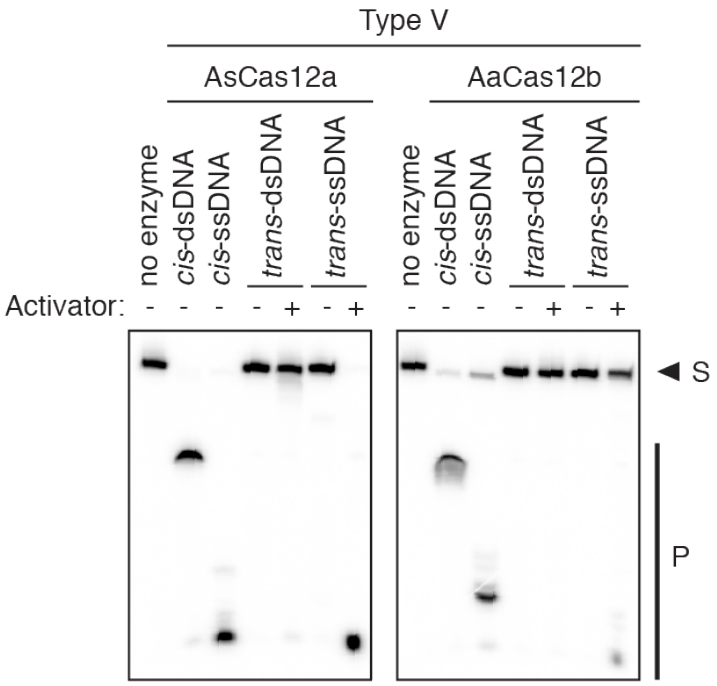



**Fig. S9**

**Activator-dependent, non-specific ssDNA cleavage activity is conserved across type V CRISPR interference proteins.** Radiolabeled *cis* (complementary) or *trans* (non-complementary) substrates were incubated with Cas12-crRNA in the presence or absence of a ssDNA activator for 30 min at 37°C (or 47.5°C for AaCas12b). For *cis*-dsDNA, non-target strand is 5' end labeled, while the target strand (complementary to guide RNA) is 5' end labeled for *cis*-ssDNA; *trans*-ssDNA and dsDNA are non-specific DNAs. In "no enzyme" lanes, 5' end labeled *trans*-ssDNA is loaded. Substrate (S) and nucleotide products (P) are resolved by denaturing PAGE.

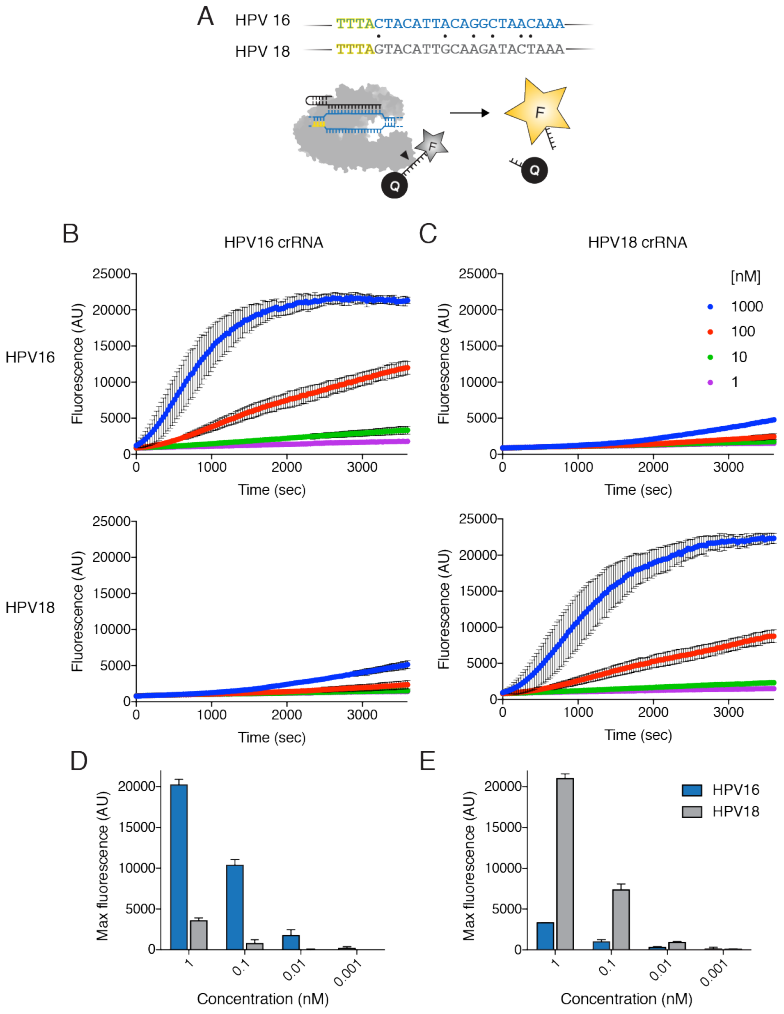



**Fig. S10**

**Cas12a distinguishes two closely related HPV sequences.** (**A**) Alignment of 20nt targeting sequences within HPV16 and HPV18 genomes that differ by 6 nucleotides, with a schematic of Cas12a detection using a ssDNA-FQ reporter. Fluorescence timecourses with LbCas12a preassembled with a crRNA targeting (**B**) HPV16 or (**C**) HPV16 in the presence of a dsDNA plasmid containing an HPV16 (top row) or HPV18 (middle row) genomic fragment and DNaseAlert substrate, with fluorescence measurements taken every 30 seconds for 1h at 37°C. (**D**) Maximum fluorescence signal obtained from timecourses in (**B**) and (**C**). Error bars represent mean ± s.d., where $n = 3$ replicates.

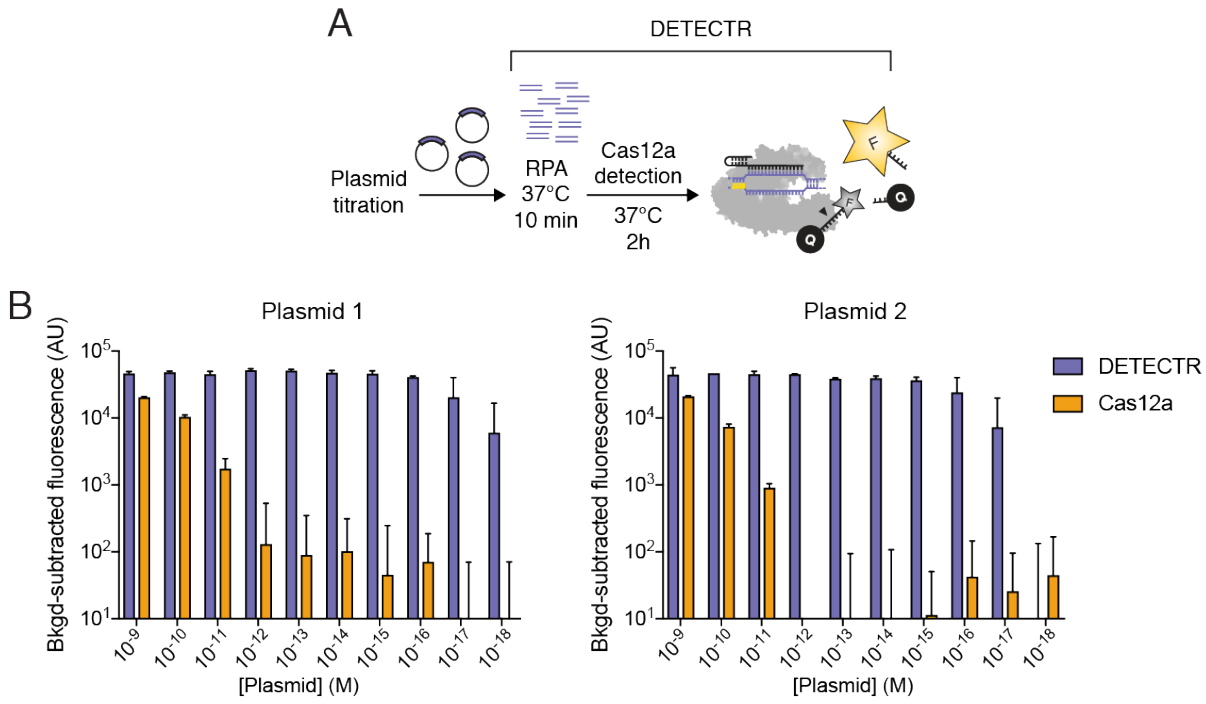



**Fig. S11**

**Isothermal amplification coupled with Cas12a detection yields DETECTR, which achieves attomolar sensitivity.** (**A**) Schematic of DETECTR, consisting of isothermal amplification by RPA and Cas12a detection using a ssDNA-FQ reporter. (**B**) Titration of two independent plasmids detected by DETECTR or Cas12a alone. Note that DETECTR achieves attomolar sensitivity. Error bars represent mean ± s.d., where $n$ = 3 replicates.

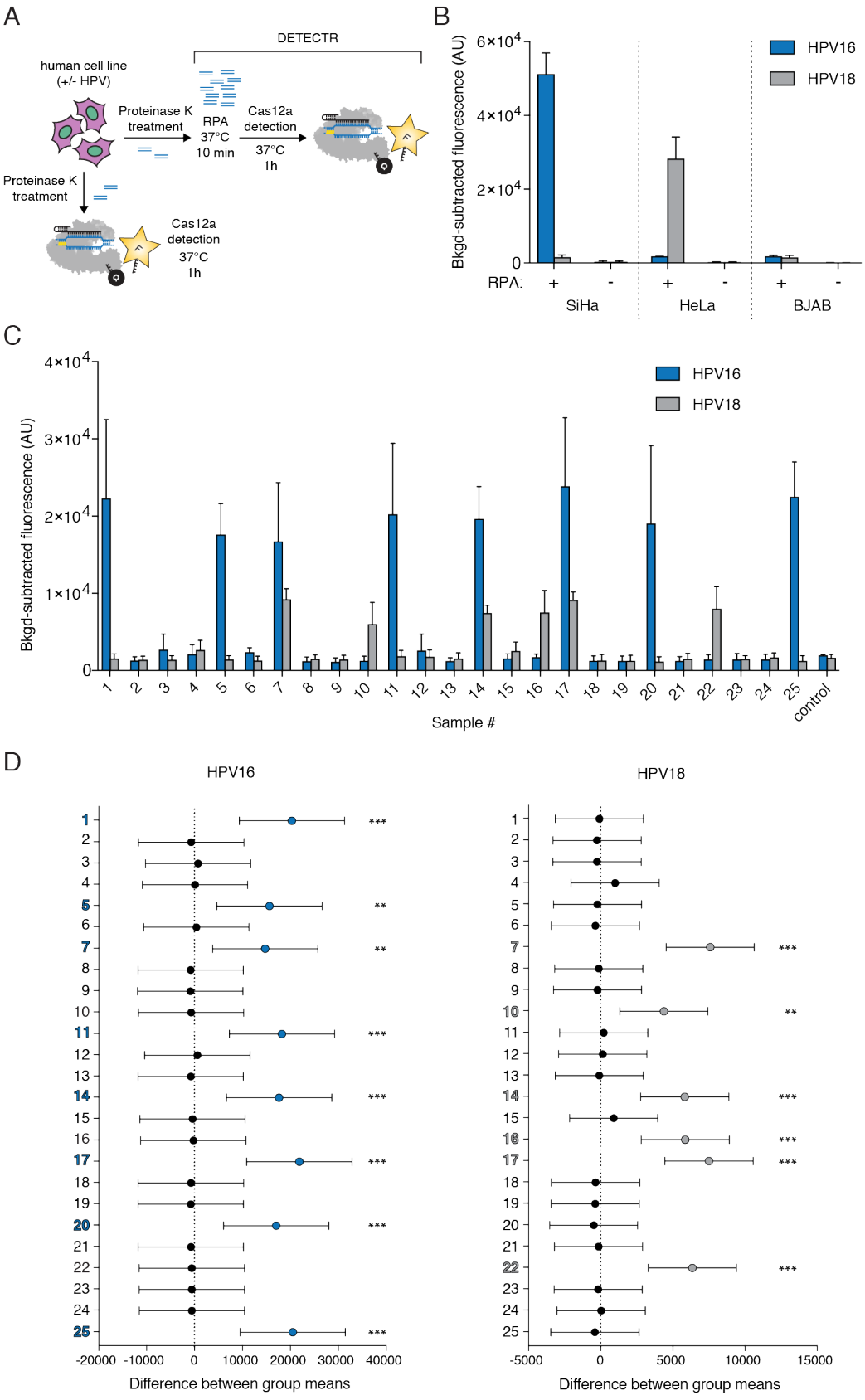

A
DETECTR
human cell line
(+/- HPV)
Proteinase K
treatment
RPA
37°C
10 min
Cas12a
detection
37°C
1h
Proteinase K
treatment
Cas12a
detection
37°C
1h
B
Bkgd-subtracted fluorescence (AU)
6×10^4
4×10^4
2×10^4
0
HPV16
HPV18
RPA:
+
-
+
-
+
-
SiHa
HeLa
BJAB
C
Bkgd-subtracted fluorescence (AU)
4×10^4
3×10^4
2×10^4
1×10^4
0
HPV16
HPV18
1
2
3
4
5
6
7
8
9
10
11
12
13
14
15
16
17
18
19
20
21
22
23
24
25
control
Sample #
D
HPV16
HPV18
***
**
**
***
***
***
***
***
**
***
***
***
***
-20000
-10000
0
10000
20000
30000
40000
-5000
0
5000
10000
15000
Difference between group means
Difference between group means

**Fig. S12**

**Identification of HPV types 16 and 18 in human cell lines and patient samples by DETECTR.** (**A**) Schematic of HPV detection by DETECTR or Cas12a alone. (**B**) Detection of HPV types 16 or 18 in SiHa (integrated HPV16), HeLa (integrated HPV18) and BJAB (no HPV) human cell lines, with or without RPA amplification. (**C**) Detection of HPV types 16 or 18 by DETECTR in 25 human anal clinical samples; BJAB cell line (no HPV) used as a control. The absence of fluorescence signal in specimens that were not infected with HPV types 16 or 18, but did contain other HPV types, was an indicator of good specificity by DETECTR. Error bars represent mean ± s.d., where $n = 3$ replicates. (**D**) Plot of 95% confidence intervals of difference between control and sample groups, based on a one-way ANOVA with Dunnett's post test, where $n = 3$ replicates. Highlighted sample numbers indicate positive detection of HPV16 (left) or HPV18 (right) in patient samples, where $^{**}p \leq 0.01$ and $^{***}p \leq 0.001$.

A

| # | 16 | 18 | HPV types |
|---|---|---|---|
| 1 | 2 | 0 | 16 |
| 2 | 0 | 0 | - |
| 3 | 0 | 0 | 32/42 |
| 4 | 0 | 1 | 18 |
| 5 | 2 | 0 | 16 90/106 |
| 6 | 0 | 0 | 35 |
| 7 | 1 | 2 | 16 18 |
| 8 | 0 | 0 | 31 35 |
| 9 | 0 | 0 | - |
| 10 | 0 | 4 | 6/11 18 26/69 58 70 84 Mix1 |
| 11 | 4 | 0 | 6/11 16 31 33 51 59 82+ 84 90/106 102/89 Mix1 |
| 12 | 0 | 0 | 56 Mix1 |
| 13 | 0 | 0 | - |
| 14 | 3 | 3 | 16 18 53 58 |
| 15 | 0 | 0 | - |
| 16 | 0 | 2 | 6/11 18 30 51 53 70 |
| 17 | 4 | 4 | 16 18 39 53 56 68 |
| 18 | 0 | 0 | - |
| 19 | 0 | 0 | 31 Mix1 |
| 20 | 4 | 0 | 16 33 83 102/89 |
| 21 | 0 | 0 | 6/11 |
| 22 | 0 | 4 | 18 33 58 |
| 23 | 0 | 0 | - |
| 24 | 0 | 1 | 6/11 18 |
| 25 | 3 | 0 | 6/11 16 39 52 62 |

B

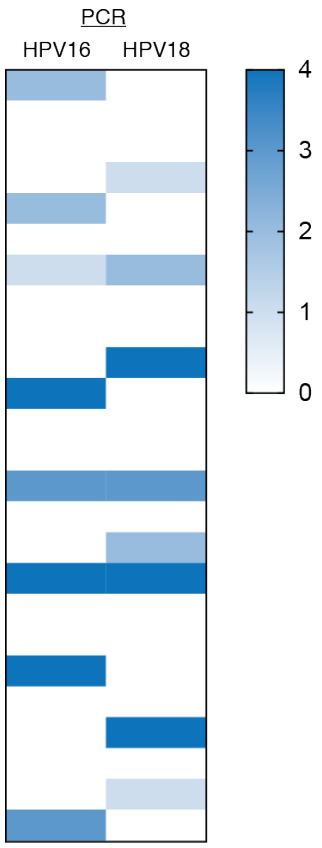



**Fig. S13**

**PCR and hybrid capture validation and genotyping of HPV in human clinical samples.** (**A**) Summary of PCR-based detection of HPV types 16 (column 2 and yellow circles) and 18 (column 3 and orange circles) and identification of other HPV types by PCR in 25 in patient samples (column 4) (*28*); subjective intensive values (0–4 scale) were assigned for each PCR-based validation (columns 2 and 3). (**B**) Heatmap depiction of PCR results.

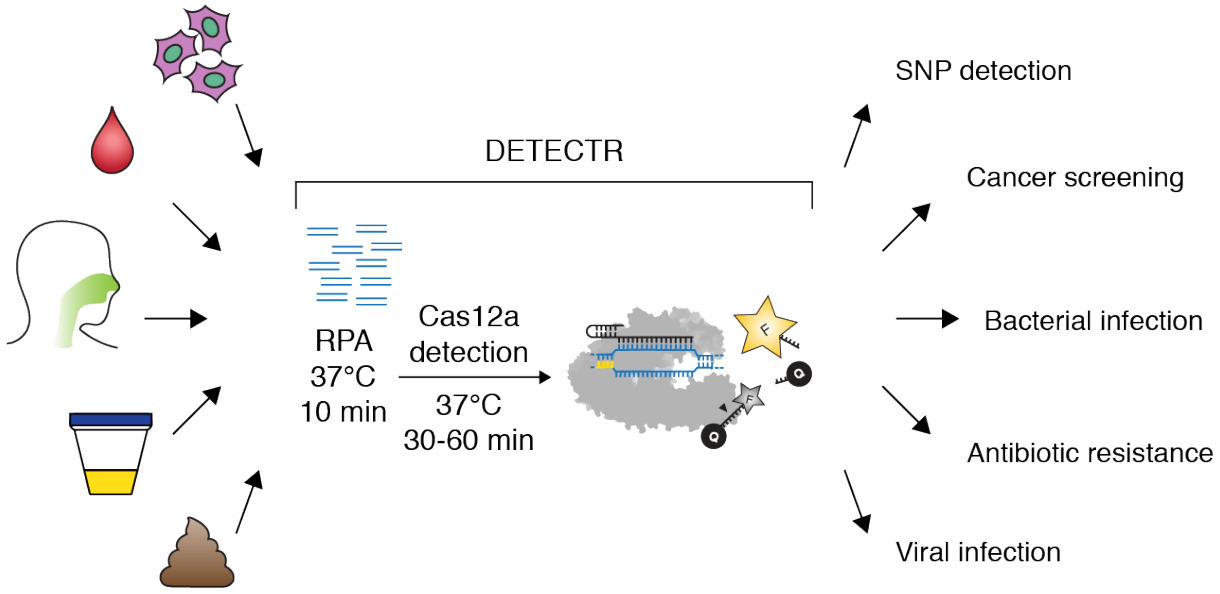



**Fig. S14**

**DETECTR as a platform for rapid, point-of-care diagnostics.** Cartoon depicting examples of clinical samples that could be used for various diagnostic applications using DETECTR.

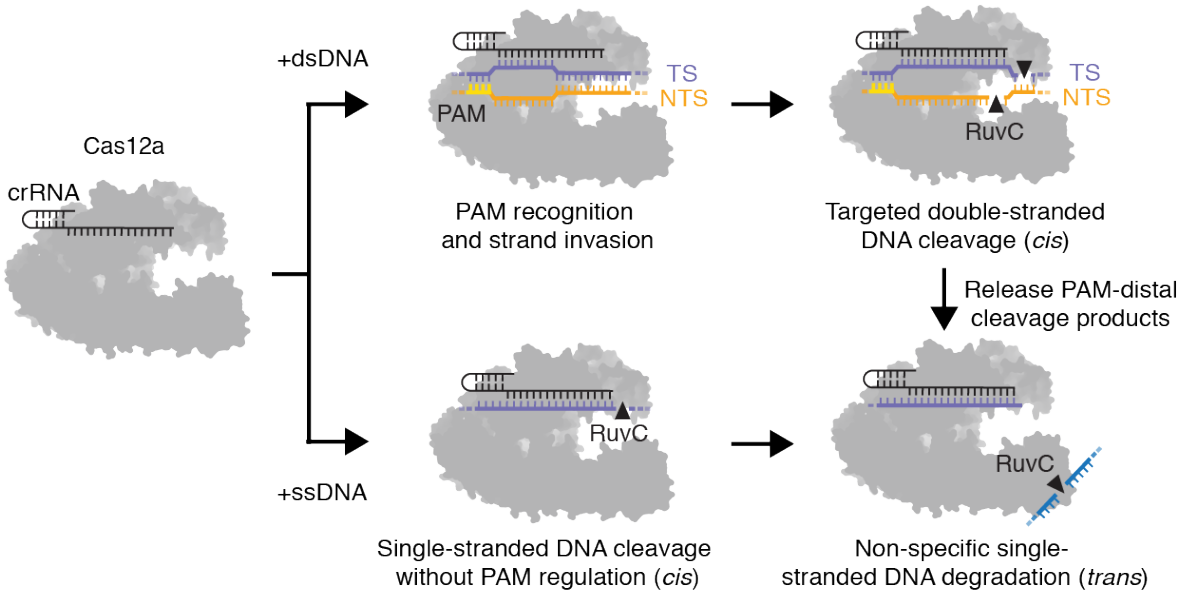



**Fig. S15**

**Model for PAM-dependent and PAM-independent activation of *cis*- and *trans*-cleavage by Cas12a.** The Cas12a-crRNA complex binds to a complementary dsDNA in a PAM-dependent manner (top) or ssDNA in a PAM-independent manner (bottom), which is sufficient to unleash indiscriminate ssDNase activity by the RuvC nuclease. Cas12a can also release its PAM-distal cleavage products, which exposes the RuvC active site for multiple rounds of non-specific ssDNA degradation.

# Supplementary Table S1

**RNA**

| | |
|---|---|
| LbCas12a crRNA - Target 1 | UAAUUUCUACUAAGUGUAGAU**CGUCGCCGUCCAGCUCGACC** |
| LbCas12a crRNA - pUC19 | UAAUUUCUACUAAGUGUAGAU**CAACGUCGUGACUGGGAAAACCCU** |
| LbCas12a crRNA - M13 | UAAUUUCUACUAAGUGUAGAU**AACGAACCACCAGCAGAAGA** |
| LbCas12a crRNA - Target 2 | UAAUUUCUACUAAGUGUAGAU**GAUCGUUACGCUAACUAUGA** |
| LbCas12a crRNA - Target 3 | UAAUUUCUACUAAGUGUAGAU**CCUGGGUGUUCCACAGCUGA** |
| LbCas12a crRNA - Plasmid 1 | UAAUUUCUACUAAGUGUAGAU**CUACAUUACAGGCUAACAAA** |
| LbCas12a crRNA - Plasmid 2 | UAAUUUCUACUAAGUGUAGAU**GUACAUUGCAAGAUACUAAA** |
| LbCas12a crRNA - HPV16-L1 | UAAUUUCUACUAAGUGUAGAU**UGAAGUAGAUAUGGCAGCAC** |
| LbCas12a crRNA - HPV18-L1 | UAAUUUCUACUAAGUGUAGAU**ACAAUAUGUGCUUCUACACA** |
| AsCas12a crRNA - Target 2 | UAAUUUCUACUCUUGUAGAU**GAUCGUUACGCUAACUAUGA** |
| FnCas12a crRNA - Target 2 | UAAUUUCUACUGUUGUAGAU**GAUCGUUACGCUAACUAUGA** |
| AaCas12b crRNA - Target 2 | GUCUAGAGGACAGAAUUUUUCAACGGGUGUGCCAAUGGCCACUUUCCAGGUGGCAAAGCCCGUUGAGCUUCUCAAAUCUGAGAAGUGGCAC**GAUCGUUACGCUAACUAUGA** |
| SpCas9 sgRNA - Target 1 | **CGUCGCCGUCCAGCUCGACC**GUUUUAGAGCUAUGCUGUUUUGGAAACAAAACAGCAUAGCAAGUUAAAAUAAGGCUAGUCCGUUAUCAACUUGAAAAAGUGGCACCGAGUCGGUGC |
| SpCas9 sgRNA - M13 | **AACGAACCACCAGCAGAAGA**GUUUUAGAGCUAUGCUGUUUUGGAAACAAAACAGCAUAGCAAGUUAAAAUAAGGCUAGUCCGUUAUCAACUUGAAAAAGUGGCACCGAGUCGGUGC |
| SpCas9 sgRNA - Target 2 | **GAUCGUUACGCUAACUAUGA**GUUUUAGAGCUAUGCUGUUUUGGAAACAAAACAGCAUAGCAAGUUAAAAUAAGGCUAGUCCGUUAUCAACUUGAAAAAGUGGCACCGAGUCGGUGC |
| NmCas9 sgRNA - Target 2 | **GAUCGUUACGCUAACUAUGA**GUUGUAGCUCCCUUUCUCAUUUCGCAGUGCGAAAGCACUGCGAAAUGAGAACCGUUGCUACAAUAAGGCCGUCUGAAAAGAUGUGCCGCAACGCUCUGCCCCUUAAAGCUUCUGC |
| CjCas9 sgRNA - Target 2 | **GAUCGUUACGCUAACUAUGA**GUUUUAGUCCCUUUUUAAAUUUCUUUAUGGUAAAAUUAUAAUCUCAUAAGAAAUUUAAAAAGGGACUAAAAUAAAGAGUUUGCGGGACUCUGCGGGGUUACAAUCCCCUAAAACCGCUU |
| Target 1 ssRNA | GCCGGGGUGGUGCCCAUCCUGGUCGAGCUGGACGGCGACGUAAACGGCCACAAGC |
| Target 2 ssRNA | UAGCAUUCCACAGACAGCCCUCAUAGUUAGCGUAACGAUCUAAAGUUUUGUCGUC |

**Plasmids**

| | |
|---|---|
| M13mp18 ssDNA phage | https://benchling.com/s/seq-mnJjAqQ9tHfSPbKTNIPT |
| pUC19 dsDNA plasmid | https://benchling.com/s/seq-x4orD9lwDx2iHa6Ns3pR |
| Plasmid 1 | https://benchling.com/s/seq-g0t5PySBcx4cwnz2h82w |
| Plasmid 2 | https://benchling.com/s/seq-hv244BG5z20ON23SUZwq |

**DNA**

| | |
|---|---|
| non-specific NTS | AGCTTGTCTGCCATGGACATGCAGACTATACTGTTATTGTTGTACAGACCGAATTCCC |
| non-specific TS | GGGAATTCGGTCTGTACAACAATAACAGTATAGTCTGCATGTCCATGGCAGACAAGCT |
| | |
| Target 1_NTS | GCTTGTGGCCGTTTA**CGTCGCCGTCCAGCTCGACC**AGGATGGGCACCACCCCGGC |
| Target 1_TS | GCCGGGGTGGTGCCCATCCT**GGTCGAGCTGGACGGCGACG**TAAACGGCCACAAGC |
| Target 1_20-19_NTS | GCTTGTGGCCGTTTA**CGTCGCCGTCCAGCTCGA**GGAGGATGGGCACCACCCCGGC |
| Target 1_20-19_TS | GCCGGGGTGGTGCCCATCCTCC**TCGAGCTGGACGGCGACG**TAAACGGCCACAAGC |
| Target 1_18-17_NTS | GCTTGTGGCCGTTTA**CGTCGCCGTCCAGCTCCT**CCAGGATGGGCACCACCCCGGC |
| Target 1_18-17_TS | GCCGGGGTGGTGCCCATCCT**GGAGGAGCTGGACGGCGACG**TAAACGGCCACAAGC |
| Target 1_16-15_NTS | GCTTGTGGCCGTTTA**CGTCGCCGTCCAGCAGGACC**AGGATGGGCACCACCCCGGC |
| Target 1_16-15_TS | GCCGGGGTGGTGCCCATCCT**GGTCCTGCTGGACGGCGACG**TAAACGGCCACAAGC |
| Target 1_14-13_NTS | GCTTGTGGCCGTTTA**CGTCGCCGTCCACGTCGACC**AGGATGGGCACCACCCCGGC |
| Target 1_14-13_TS | GCCGGGGTGGTGCCCATCCT**GGTCGACGTGGACGGCGACG**TAAACGGCCACAAGC |
| Target 1_12-11_NTS | GCTTGTGGCCGTTTA**CGTCGCCGTCGTGCTCGACC**AGGATGGGCACCACCCCGGC |
| Target 1_12-11_TS | GCCGGGGTGGTGCCCATCCT**GGTCGAGCACGACGGCGACG**TAAACGGCCACAAGC |
| Target 1_10-9_NTS | GCTTGTGGCCGTTTA**CGTCGCCGAGCAGCTCGACC**AGGATGGGCACCACCCCGGC |
| Target 1_10-9_TS | GCCGGGGTGGTGCCCATCCT**GGTCGAGCTGCTCGGCGACG**TAAACGGCCACAAGC |
| Target 1_8-7_NTS | GCTTGTGGCCGTTTA**CGTCGCGCTCCAGCTCGACC**AGGATGGGCACCACCCCGGC |
| Target 1_8-7_TS | GCCGGGGTGGTGCCCATCCT**GGTCGAGCTGGAGCGCGACG**TAAACGGCCACAAGC |
| Target 1_6-5_NTS | GCTTGTGGCCGTTTA**CGTCCGCGTCCAGCTCGACC**AGGATGGGCACCACCCCGGC |
| Target 1_6-5_TS | GCCGGGGTGGTGCCCATCCT**GGTCGAGCTGGACGCGGACG**TAAACGGCCACAAGC |
| Target 1_4-3_NTS | GCTTGTGGCCGTTTA**CGAGGCCGTCCAGCTCGACC**AGGATGGGCACCACCCCGGC |
| Target 1_4-3_TS | GCCGGGGTGGTGCCCATCCT**GGTCGAGCTGGACGGCCTCG**TAAACGGCCACAAGC |
| Target 1_2-1_NTS | GCTTGTGGCCGTTTA**GCTCGCCGTCCAGCTCGACC**AGGATGGGCACCACCCCGGC |
| Target 1_2-1_TS | GCCGGGGTGGTGCCCATCCT**GGTCGAGCTGGACGGCGAGC**TAAACGGCCACAAGC |
| Target 1_mut-PAM_NTS | GCTTGTGGCCGAGCA**CGTCGCCGTCCAGCTCGACC**AGGATGGGCACCACCCCGGC |
| Target 1_mut-PAM_TS | GCCGGGGTGGTGCCCATCCT**GGTCGAGCTGGACGGCGACG**TGCTCGGCCACAAGC |
| | |
| Target 1_5nt_TS | **CGACG**TAAACGGCCACAAGC |
| Target 1_10nt_TS | **GACGGCGACG**TAAACGGCCACAAGC |
| Target 1_15nt_TS | **AGCTGGACGGCGACG**TAAACGGCCACAAGC |
| Target 1_20nt_TS | **GGTCGAGCTGGACGGCGACG**TAAACGGCCACAAGC |
| Target 1_25nt_TS | ATCCT**GGTCGAGCTGGACGGCGACG**TAAACGGCCACAAGC |
| | |
| Target 1_5nt_NTS | GCTTGTGGCCGTTTA**CGTCG** |
| Target 1_10nt_NTS | GCTTGTGGCCGTTTA**CGTCGCCGTC** |
| Target 1_15nt_NTS | GCTTGTGGCCGTTTA**CGTCGCCGTCCAGCT** |
| Target 1_20nt_NTS | GCTTGTGGCCGTTTA**CGTCGCCGTCCAGCTCGACC** |
| Target 1_25nt_NTS | GCTTGTGGCCGTTTA**CGTCGCCGTCCAGCTCGACC**AGGAT |

| | |
|---|---|
| Target 2_NTS | GACGACAAAACTTTAGATCGTTACGCTAACTATGAGGGCTGTCTGTGGAATGCTA |
| Target 2_TS | TAGCATTCCACAGACAGCCCTCATAGTTAGCGTAACGATCTAAAGTTTTGTCGTC |
| Target 2_20-19_NTS | GACGACAAAACTTTAGATCGTTACGCTAACTATCTGGGCTGTCTGTGGAATGCTA |
| Target 2_20-19_TS | TAGCATTCCACAGACAGCCCAGATAGTTAGCGTAACGATCTAAAGTTTTGTCGTC |
| Target 2_18-17_NTS | GACGACAAAACTTTAGATCGTTACGCTAACTTAGAGGGCTGTCTGTGGAATGCTA |
| Target 2_18-17_TS | TAGCATTCCACAGACAGCCCTCTAAGTTAGCGTAACGATCTAAAGTTTTGTCGTC |
| Target 2_16-15_NTS | GACGACAAAACTTTAGATCGTTACGCTAAGAATGAGGGCTGTCTGTGGAATGCTA |
| Target 2_16-15_TS | TAGCATTCCACAGACAGCCCTCATTCTTAGCGTAACGATCTAAAGTTTTGTCGTC |
| Target 2_14-13_NTS | GACGACAAAACTTTAGATCGTTACGCTTTCTATGAGGGCTGTCTGTGGAATGCTA |
| Target 2_14-13_TS | TAGCATTCCACAGACAGCCCTCATAGAAAGCGTAACGATCTAAAGTTTTGTCGTC |
| Target 2_12-11_NTS | GACGACAAAACTTTAGATCGTTACGGAAACTATGAGGGCTGTCTGTGGAATGCTA |
| Target 2_12-11_TS | TAGCATTCCACAGACAGCCCTCATAGTTTCCGTAACGATCTAAAGTTTTGTCGTC |
| Target 2_10-9_NTS | GACGACAAAACTTTAGATCGTTAGCCTAACTATGAGGGCTGTCTGTGGAATGCTA |
| Target 2_10-9_TS | TAGCATTCCACAGACAGCCCTCATAGTTAGGCTAACGATCTAAAGTTTTGTCGTC |
| Target 2_8-7_NTS | GACGACAAAACTTTAGATCGTATCGCTAACTATGAGGGCTGTCTGTGGAATGCTA |
| Target 2_8-7_TS | TAGCATTCCACAGACAGCCCTCATAGTTAGCGATACGATCTAAAGTTTTGTCGTC |
| Target 2_6-5_NTS | GACGACAAAACTTTAGATCCATACGCTAACTATGAGGGCTGTCTGTGGAATGCTA |
| Target 2_6-5_TS | TAGCATTCCACAGACAGCCCTCATAGTTAGCGTATGGATCTAAAGTTTTGTCGTC |
| Target 2_4-3_NTS | GACGACAAAACTTTAGAAGGTTACGCTAACTATGAGGGCTGTCTGTGGAATGCTA |
| Target 2_4-3_TS | TAGCATTCCACAGACAGCCCTCATAGTTAGCGTAACCTTCTAAAGTTTTGTCGTC |
| Target 2_2-1_NTS | GACGACAAAACTTTACTTCGTTACGCTAACTATGAGGGCTGTCTGTGGAATGCTA |
| Target 2_2-1_TS | TAGCATTCCACAGACAGCCCTCATAGTTAGCGTAACGAAGTAAAGTTTTGTCGTC |
| Target 2_mut-PAM_NTS | GACGACAAAACAGCAGATCGTTACGCTAACTATGAGGGCTGTCTGTGGAATGCTA |
| Target 2_mut-PAM_TS | TAGCATTCCACAGACAGCCCTCATAGTTAGCGTAACGATCTGCTGTTTTGTCGTC |
| Target 2_NmCas9_NTS | GACGACAAAACTTTAGATCGTTACGCTAACTATGAGGGCGAGTTGTGGAATGCTA |
| Target 2_NmCas9_TS | TAGCATTCCACAACTCGCCCTCATAGTTAGCGTAACGATCTAAAGTTTTGTCGTC |
| Target 2_CjCas9_TS | GACGACAAAACTTTAGATCGTTACGCTAACTATGAGGGCCAAATGTGGAATGCTA |
| Target 2_CjCas9_TS | TAGCATTCCACATTTGGCCCTCATAGTTAGCGTAACGATCTAAAGTTTTGTCGTC |
| | |
| Target 3_NTS | AGTTGTGTTAGTTTACCTGGGTGTTCCACAGCTGATAGTGATTGCCTTGAATAAA |
| Target 3_TS | TTTATTCAAGGCAATCACTATCAGCTGTGGAACACCCAGGTAAACTAACACAACT |
| Target 3_20-19_NTS | AGTTGTGTTAGTTTACCTGGGTGTTCCACAGCTCTAGTGATTGCCTTGAATAAA |
| Target 3_20-19_TS | TTTATTCAAGGCAATCACTAAGAGCTGTGGAACACCCAGGTAAACTAACACAACT |
| Target 3_18-17_NTS | AGTTGTGTTAGTTTACCTGGGTGTTCCACAGGAGATAGTGATTGCCTTGAATAAA |
| Target 3_18-17_TS | TTTATTCAAGGCAATCACTATCTCCTGTGGAACACCCAGGTAAACTAACACAACT |
| Target 3_16-15_NTS | AGTTGTGTTAGTTTACCTGGGTGTTCCACTCCTGATAGTGATTGCCTTGAATAAA |
| Target 3_16-15_TS | TTTATTCAAGGCAATCACTATCAGGAGTGGAACACCCAGGTAAACTAACACAACT |
| Target 3_14-13_NTS | AGTTGTGTTAGTTTACCTGGGTGTTCCTGAGCTGATAGTGATTGCCTTGAATAAA |
| Target 3_14-13_TS | TTTATTCAAGGCAATCACTATCAGCTCAGGAACACCCAGGTAAACTAACACAACT |
| Target 3_12-11_NTS | AGTTGTGTTAGTTTACCTGGGTGTTGGACAGCTGATAGTGATTGCCTTGAATAAA |
| Target 3_12-11_TS | TTTATTCAAGGCAATCACTATCAGCTGTCCAACACCCAGGTAAACTAACACAACT |
| Target 3_10-9_NTS | AGTTGTGTTAGTTTACCTGGGTGAACCACAGCTGATAGTGATTGCCTTGAATAAA |
| Target 3_10-9_TS | TTTATTCAAGGCAATCACTATCAGCTGTGGTTCACCCAGGTAAACTAACACAACT |
| Target 3_8-7_NTS | AGTTGTGTTAGTTTACCTGGGACTTCCACAGCTGATAGTGATTGCCTTGAATAAA |
| Target 3_8-7_TS | TTTATTCAAGGCAATCACTATCAGCTGTGGAAGTCCCAGGTAAACTAACACAACT |
| Target 3_6-5_NTS | AGTTGTGTTAGTTTACCTGCCTGTTCCACAGCTGATAGTGATTGCCTTGAATAAA |
| Target 3_6-5_TS | TTTATTCAAGGCAATCACTATCAGCTGTGGAACAGGCAGGTAAACTAACACAACT |
| Target 3_4-3_NTS | AGTTGTGTTAGTTTACCACGGTGTTCCACAGCTGATAGTGATTGCCTTGAATAAA |
| Target 3_4-3_TS | TTTATTCAAGGCAATCACTATCAGCTGTGGAACACCGTGGTAAACTAACACAACT |
| Target 3_2-1_NTS | AGTTGTGTTAGTTTAGGTGGGTGTTCCACAGCTGATAGTGATTGCCTTGAATAAA |
| Target 3_2-1_TS | TTTATTCAAGGCAATCACTATCAGCTGTGGAACACCCACCTAAACTAACACAACT |
| Target 3_mut-PAM_NTS | AGTTGTGTTAGAGCACCTGGGTGTTCCACAGCTGATAGTGATTGCCTTGAATAAA |
| Target 3_mut-PAM_TS | TTTATTCAAGGCAATCACTATCAGCTGTGGAACACCCAGGTGCTCTAACACAACT |

**FQ substrates**

| | |
|---|---|
| ssDNA-FQ reporter | /56-FAM/TTATT/3IABkFQ/ |
| ssRNA-FQ reporter | /56-FAM/rUrUrArUrU/3IABkFQ/ |
| Dnase-Alert substrate (IDT) | Proprietary |

**RPA primers**

| | |
|---|---|
| Plasmid 1_F | GCAAACCACCTATAGGGGAACAC |
| Plasmid 1_R | CAGCCAACTCAGCTTCCTTTC |
| Plasmid 2_F | CATGCCGCCACGTCTAATGTTTC |
| Plasmid 2_R | GGTGAAGCACGCATACCTGTG |
| HPV16-L1_F | TTGTTGGGGTAACCAACTATTTGTTACTGTT |
| HPV16-L1_R | CCTCCCCATGTCTGAGGTACTCCTTAAAG |
| HPV18-L1_F | GCATAATCAATTATTTGTTACTGTGGTAGATACCACT |
| HPV18-L1-R | GCTATACTGCTTAAATTTGGTAGCATCATATTGC |

# Table S1

## Nucleic acids used in this study.

**References**


1. R. Barrangou, C. Fremaux, H. Deveau, M. Richards, P. Boyaval, S. Moineau, D. A. Romero, P. Horvath, CRISPR provides acquired resistance against viruses in prokaryotes. *Science* **315**, 1709–1712 (2007). doi:10.1126/science.1138140 Medline

2. L. A. Marraffini, E. J. Sontheimer, CRISPR interference limits horizontal gene transfer in staphylococci by targeting DNA. *Science* **322**, 1843–1845 (2008). doi:10.1126/science.1165771 Medline

3. E. V. Koonin, K. S. Makarova, F. Zhang, Diversity, classification and evolution of CRISPR-Cas systems. *Curr. Opin. Microbiol.* **37**, 67–78 (2017). doi:10.1016/j.mib.2017.05.008 Medline

4. J. A. Doudna, E. Charpentier, The new frontier of genome engineering with CRISPR-Cas9. *Science* **346**, 1258096 (2014). doi:10.1126/science.1258096 Medline

5. R. Barrangou, P. Horvath, A decade of discovery: CRISPR functions and applications. *Nat. Microbiol.* **2**, 17092 (2017). doi:10.1038/nmicrobiol.2017.92 Medline

6. M. Jinek, K. Chylinski, I. Fonfara, M. Hauer, J. A. Doudna, E. Charpentier, A programmable dual-RNA–guided DNA endonuclease in adaptive bacterial immunity. *Science* **337**, 816–821 (2012). doi:10.1126/science.1225829 Medline

7. J. S. Chen, J. A. Doudna, The chemistry of Cas9 and its CRISPR colleagues. *Nat. Rev. Chem.* **1**, 0078 (2017). doi:10.1038/s41570-017-0078

8. B. Zetsche, J. S. Gootenberg, O. O. Abudayyeh, I. M. Slaymaker, K. S. Makarova, P. Essletzbichler, S. E. Volz, J. Joung, J. van der Oost, A. Regev, E. V. Koonin, F. Zhang, Cpf1 is a single RNA-guided endonuclease of a class 2 CRISPR-Cas system. *Cell* **163**, 759–771 (2015). doi:10.1016/j.cell.2015.09.038 Medline

9. D. C. Swarts, J. van der Oost, M. Jinek, Structural basis for guide RNA processing and seed-dependent DNA targeting by CRISPR-Cas12a. *Mol. Cell* **66**, 221–233.e4 (2017). doi:10.1016/j.molcel.2017.03.016 Medline

10. D. Dong, K. Ren, X. Qiu, J. Zheng, M. Guo, X. Guan, H. Liu, N. Li, B. Zhang, D. Yang, C. Ma, S. Wang, D. Wu, Y. Ma, S. Fan, J. Wang, N. Gao, Z. Huang, The crystal structure of Cpf1 in complex with CRISPR RNA. *Nature* **532**, 522–526 (2016). doi:10.1038/nature17944 Medline

11. P. Gao, H. Yang, K. R. Rajashankar, Z. Huang, D. J. Patel, Type V CRISPR-Cas Cpf1 endonuclease employs a unique mechanism for crRNA-mediated target DNA recognition. *Cell Res.* **26**, 901–913 (2016). doi:10.1038/cr.2016.88 Medline

12. S. Stella, P. Alcón, G. Montoya, Structure of the Cpf1 endonuclease R-loop complex after target DNA cleavage. *Nature* **546**, 559–563 (2017). Medline

13. T. Yamano, H. Nishimasu, B. Zetsche, H. Hirano, I. M. Slaymaker, Y. Li, I. Fedorova, T. Nakane, K. S. Makarova, E. V. Koonin, R. Ishitani, F. Zhang, O. Nureki, Crystal structure of Cpf1 in complex with guide RNA and target DNA. *Cell* **165**, 949–962 (2016). doi:10.1016/j.cell.2016.04.003 Medline

14. I. Fonfara, H. Richter, M. Bratovič, A. Le Rhun, E. Charpentier, The CRISPR-associated DNA-cleaving enzyme Cpf1 also processes precursor CRISPR RNA. *Nature* **532**, 517–521 (2016). doi:10.1038/nature17945 Medline

15. B. Zetsche, M. Heidenreich, P. Mohanraju, I. Fedorova, J. Kneppers, E. M. DeGennaro, N. Winblad, S. R. Choudhury, O. O. Abudayyeh, J. S. Gootenberg, W. Y. Wu, D. A. Scott, K. Severinov, J. van der Oost, F. Zhang, Multiplex gene editing by CRISPR-Cpf1 using a single crRNA array. *Nat. Biotechnol.* **35**, 31–34 (2017). doi:10.1038/nbt.3737 Medline

16. X. Tang, L. G. Lowder, T. Zhang, A. A. Malzahn, X. Zheng, D. F. Voytas, Z. Zhong, Y. Chen, Q. Ren, Q. Li, E. R. Kirkland, Y. Zhang, Y. Qi, A CRISPR-Cpf1 system for efficient genome editing and transcriptional repression in plants. *Nat. Plants* **3**, 17018 (2017). doi:10.1038/nplants.2017.18 Medline

17. Y. Zhang, R. Rajan, H. S. Seifert, A. Mondragón, E. J. Sontheimer, DNase H activity of *Neisseria meningitidis* Cas9. *Mol. Cell* **60**, 242–255 (2015). doi:10.1016/j.molcel.2015.09.020 Medline

18. E. Ma, L. B. Harrington, M. R. O'Connell, K. Zhou, J. A. Doudna, Single-stranded DNA cleavage by divergent CRISPR-Cas9 enzymes. *Mol. Cell* **60**, 398–407 (2015). doi:10.1016/j.molcel.2015.10.030 Medline

19. A. East-Seletsky, M. R. O'Connell, S. C. Knight, D. Burstein, J. H. D. Cate, R. Tjian, J. A. Doudna, Two distinct RNase activities of CRISPR-C2c2 enable guide-RNA processing and RNA detection. *Nature* **538**, 270–273 (2016). doi:10.1038/nature19802 Medline

20. D. Singh, J. Mallon, A. Poddar, Y. Wang, R. Tipanna, O. Yang, S. Bailey, T. Ha, Real-time observation of DNA target interrogation and product release by the RNA-guided endonuclease CRISPR Cpf1. BioRxiv 205575 [Preprint]. 18 October 2017. https://doi.org/10.1101/205575

21. R. A. Alberty, G. G. Hammes, Application of the theory of diffusion-controlled reactions to enzyme kinetics. *J. Phys. Chem.* **62**, 154–159 (1958). doi:10.1021/j150560a005

22. D. Kim, J. Kim, J. K. Hur, K. W. Been, S. H. Yoon, J.-S. Kim, Genome-wide analysis reveals specificities of Cpf1 endonucleases in human cells. *Nat. Biotechnol.* **34**, 863–868 (2016). doi:10.1038/nbt.3609 Medline

23. B. P. Kleinstiver, S. Q. Tsai, M. S. Prew, N. T. Nguyen, M. M. Welch, J. M. Lopez, Z. R. McCaw, M. J. Aryee, J. K. Joung, Genome-wide specificities of CRISPR-Cas Cpf1 nucleases in human cells. *Nat. Biotechnol.* **34**, 869–874 (2016). doi:10.1038/nbt.3620 Medline

24. S. Shmakov, A. Smargon, D. Scott, D. Cox, N. Pyzocha, W. Yan, O. O. Abudayyeh, J. S. Gootenberg, K. S. Makarova, Y. I. Wolf, K. Severinov, F. Zhang, E. V. Koonin, Diversity and evolution of class 2 CRISPR-Cas systems. *Nat. Rev. Microbiol.* **15**, 169–182 (2017). doi:10.1038/nrmicro.2016.184 Medline

25. J. R. Elmore, N. F. Sheppard, N. Ramia, T. Deighan, H. Li, R. M. Terns, M. P. Terns, Bipartite recognition of target RNAs activates DNA cleavage by the Type III-B CRISPR-Cas system. *Genes Dev.* **30**, 447–459 (2016). doi:10.1101/gad.272153.115 Medline

26. O. O. Abudayyeh, J. S. Gootenberg, S. Konermann, J. Joung, I. M. Slaymaker, D. B. T. Cox, S. Shmakov, K. S. Makarova, E. Semenova, L. Minakhin, K. Severinov, A. Regev, E. S. Lander, E. V. Koonin, F. Zhang, C2c2 is a single-component programmable RNA-guided RNA-targeting CRISPR effector. *Science* **353**, aaf5573 (2016). doi:10.1126/science.aaf5573 Medline

27. C. B. Woodman, S. I. Collins, L. S. Young, The natural history of cervical HPV infection: Unresolved issues. *Nat. Rev. Cancer* **7**, 11–22 (2007). doi:10.1038/nrc2050 Medline

28. J. M. Palefsky, E. A. Holly, M. L. Ralston, N. Jay, Prevalence and risk factors for human papillomavirus infection of the anal canal in human immunodeficiency virus (HIV)-positive and HIV-negative homosexual men. *J. Infect. Dis.* **177**, 361–367 (1998). doi:10.1086/514194 Medline

29. J. S. Gootenberg, O. O. Abudayyeh, J. W. Lee, P. Essletzbichler, A. J. Dy, J. Joung, V. Verdine, N. Donghia, N. M. Daringer, C. A. Freije, C. Myhrvold, R. P. Bhattacharyya, J. Livny, A. Regev, E. V. Koonin, D. T. Hung, P. C. Sabeti, J. J. Collins, F. Zhang, Nucleic acid detection with CRISPR-Cas13a/C2c2. *Science* **356**, 438–442 (2017). doi:10.1126/science.aam9321 Medline

30. P. Samai, N. Pyenson, W. Jiang, G. W. Goldberg, A. Hatoum-Aslan, L. A. Marraffini, Co-transcriptional DNA and RNA cleavage during type III CRISPR-Cas immunity. *Cell* **161**, 1164–1174 (2015). doi:10.1016/j.cell.2015.04.027 Medline

31. J. M. Sogo, M. Lopes, M. Foiani, Fork reversal and ssDNA accumulation at stalled replication forks owing to checkpoint defects. *Science* **297**, 599–602 (2002). doi:10.1126/science.1074023 Medline

32. V. Bhatia, E. Herrera-Moyano, A. Aguilera, B. Gómez-González, The role of replication-associated repair factors on R-loops. *Genes (Basel)* **8**, E171 (2017). doi:10.3390/genes8070171 Medline

33. Y. Zhang, Y. Feng, S. Chatterjee, S. Tuske, M. X. Ho, E. Arnold, R. H. Ebright, Structural basis of transcription initiation. *Science* **338**, 1076–1080 (2012). doi:10.1126/science.1227786 Medline

34. C. D. Richardson, G. J. Ray, M. A. DeWitt, G. L. Curie, J. E. Corn, Enhancing homology-directed genome editing by catalytically active and inactive CRISPR-Cas9 using asymmetric donor DNA. *Nat. Biotechnol.* **34**, 339–344 (2016). doi:10.1038/nbt.3481 Medline

35. M. Jinek, F. Jiang, D. W. Taylor, S. H. Sternberg, E. Kaya, E. Ma, C. Anders, M. Hauer, K. Zhou, S. Lin, M. Kaplan, A. T. Iavarone, E. Charpentier, E. Nogales, J. A. Doudna, Structures of Cas9 endonucleases reveal RNA-mediated conformational activation. *Science* **343**, 1247997 (2014). doi:10.1126/science.1247997 Medline

36. W. T. Seaman, E. Andrews, M. Couch, E. M. Kojic, S. Cu-Uvin, J. Palefsky, A. M. Deal, J. Webster-Cyriaque, Detection and quantitation of HPV in genital and oral tissues and fluids by real time PCR. *Virol. J.* **7**, 194 (2010). doi:10.1186/1743-422X-7-194 Medline

37. E. A. Morrison, G. L. Goldberg, A. S. Kadish, R. D. Burk, Polymerase chain reaction detection of human papillomavirus: Quantitation may improve clinical utility. *J. Clin. Microbiol.* **30**, 2539–2543 (1992). Medline